because failure to control the environment affects physiological activity in both the neuroendocrine and immune systems. Thus the individual may actually experience more symptoms as a function of physiological activation (*50*).
52. A. Bandura, L. Reese, N. E. Adams, *J. Pers. Soc. Psychol.* **43**, 5 (1982); J. Geer and E. Maisel, *ibid.* **23**, 314 (1972); D. C. Glass, B. Reim, J. E. Singer, *J. Exp. Soc. Psychol.* **7**, 244 (1971).
53. J. M. Weiss, *Psychosom. Med.* **32**, 397 (1970).
54. ———, *Sci. Am.* **226**, 104 (June 1972).
55. M. Frankenhaeuser, in *Emotions: Their Parameters and Measurement*, L. Levi, Ed. (Raven, New York, 1975), pp. 209–234; ———, J. Lundberg, L. Forsman, *Tech. Rep. 540*, University of Stockholm, Stockholm (1978).
56. U. Lundberg and M. Frankenhaeuser, *Biol. Psychol.* **6**, 51 (1978).
57. A. Bandura, C. B. Taylor, L. Williams, I. N. Meffort, J. D. Barchas, *J. Consult. Clin. Psychol.* **53**, 406 (1985).
58. D. S. Krantz, D. C. Glass, R. Contrada, N. E. Miller, in *The Five-Year Outlook on Science and Technology* (National Science Foundation, Government Printing Office, Washington, DC, 1981), pp. 186–225.
59. H. Davis *et al.*, *Physiol. Psychol.* **5**, 280 (1977); S. Levine and G. D. Cooper, *Physiol. Behav.* **17**, 35 (1976); Frankenhaeuser and colleagues (*55, 56*) have argued that how much a task can be controlled is a major determinant of the degree of distress experienced, whereas effort is related to how demanding the task is. In turn, effort is related to catecholamine secretion, whereas distress is related to cortisol secretion. Personal control appears to be the important modulating factor in these tasks, because it tends to reduce the negative and enhance the positive aspects of arousal, thereby changing the balance between sympathetic adrenal and pituitary adrenal activity.
60. L. S. Sklar and H. Anisman, *Science* **205**, 513 (1979); M. A. Visintainer, J. R. Volpicelli, M. E. P. Seligman, *ibid.* **216**, 437 (1982).
61. S. E. Keller, J. M. Weiss, S. J. Schleifer, N. E. Miller, M. Stein, *ibid.* **213**, 1397 (1981); R. W. Bartrop, L. Lazarus, E. Luckhurt, *Lancet* **1977-I**, 834 (1977).
62. J. Rodin, in *Aging, Control and Health* (presidential address), Eastern Psychological Association, Philadelphia, 13 April 1982.
63. M. Stein, S. Schleifer, S. Keller, in *Biological Mediators of Behavior and Disease*, S. Levy, Ed. (Elsevier/North-Holland, Amsterdam, 1982), p. 147.
64. Some health-related measures do not adequately separate the effects of illness severity from the effects of taking an active role in one's health enhancement; for example, an increased number of doctor visits may indicate that the individual has suffered an illness, or that he or she has decided to participate more actively in his or her own health care.
65. These include seeking information about hypertension or renal dialysis, remaining in programs for exercise, weight loss, and smoking cessation, and complying with recommended medical regimens involving life-style change. C. A. Chambliss and E. J. Murray, *Cognit. Theor. Res.* **3**, 349 (1979); M. M. Condiotte and E. Lichtenstein, *J. Consult. Clin. Psychol.* **49**, 648 (1981); R. K. Dishman, W. Ickes, W. P. Morgan, *J. Appl. Soc. Psychol.* **10**, 115 (1980); C. K. Ewart, C. B. Taylor, L. B. Reese, R. F. Debusk, *Am. J. Cardiol.* **51**, 1076 (1984); M. M. Manning and T. L. Wright, *J. Pers. Soc. Psychol.* **45**, 421 (1983); J. B. Toner and S. B. Manuck, *Soc. Sci. Med.* **13A**, 823 (1979); K. A. Wallston and B. S. Wallston, in *Social Psychology of Health and Illness*, G. S. Sanders, Ed. (Erlbuam, Hillsdale, NJ, 1982), pp. 65–95.
66. H. Lefcourt, *Locus of Control* (Erlbaum, Hillsdale, NJ, 1976), pp. 21–25; G. Gurin and P. Gurin, in *Economics Means for Human Needs*, B. Strumpel, Ed. (Institute for Social Research, Ann Arbor, MI, 1976), pp. 131–158.
67. D. L. Parron, F. Solomon, C. D. Jenkins, *Behavior, Health Risks, and Social Disadvantages* (National Academy Press, Washington, DC, 1982); S. L. Syme and L. F. Berkman, *Am. J. Epidemiol.* **104**, 1 (1976); A. Antonovsky, *Milbank Mem. Fund Q.* **45**, 31 (1967).
68. Supported by NIA grant AG02455. I am grateful to L. Berkman, N. Miller, and J. Rowe for their comments on an earlier draft.

Investigation of Ultrafast Phenomena in the Femtosecond Time Domain

CHARLES V. SHANK

Rapid progress has taken place in the generation and application of femtosecond optical pulses. The impact of these developments is being felt in a broad range of scientific fields, including physics, chemistry, biology, and engineering. These rapidly evolving techniques have been applied to such diverse problems as phase transitions in highly excited semiconductors, molecular photofragment spectroscopy, impulsive phonon generation in solids, and optical radar ranging through biological tissue.

PROGRESS IN THE GENERATION AND MEASUREMENT OF ultrashort optical pulses continues to be driven by innovations and enhanced capabilities. Recently optical pulses have been generated with a duration of less than 8 fsec (1 fsec = 10^{-15} second) (*1*), pressing the limits of current technology. Improvements in short-pulse dye laser design have offered new means for controlling pulse width and tunability. Femtosecond amplifiers have been developed that operate with a repetition rate of 10 kHz and yet provide sufficient intensity to generate a "white light continuum" source of femtosecond optical pulses covering the ultraviolet to near-infrared region of the spectrum (*2*). Such pulses are ideal for obtaining high-resolution time-resolved spectra.

The impact of measurements in the ultrashort time domain covers a broad range of scientific activity. Femtosecond-pulse techniques have contributed significantly to the study of the dynamical properties of molecules and solids. Optically induced phase transitions have been studied by using femtosecond pulses to monitor the dynamics of the evolution of crystal symmetry (*3*). A new technique has been developed to create images with femtosecond pulses that have been put together to make a slow-motion picture that slows the action by a factor of 10^{13} (*4*). In addition, a femtosecond optical radar has been devised that can "see" into biological tissue (*5*).

Femtosecond optical pulses have been used to create nonequilibrium, nonthermal population distributions in semiconductors (*2*). With optical pulses short enough to resolve an individual molecular vibration, it has been possible to resolve phonon dephasing by impulsive Raman scattering (*6*). The dynamics of the process of exciton ionization in a semiconductor takes place at room temperature in a few hundred femtoseconds (*2*). Femtosecond pulses have also found utility for probing high-speed electronic devices and circuits (*7, 8*). Femtosecond time-resolved measurements of molecular photofragmentation have provided the first direct measurement of the time of bond breakage in a molecule (*9*). This article will touch on some of these recent advances.

The author is the director of the Electronics Research Laboratory of AT&T Bell Laboratories, Crawfords Corner Road, Holmdel, NJ 07733.

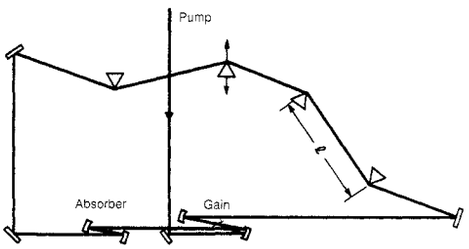

Fig. 1. The optical cavity configuration of a colliding-pulse, mode-locked dye laser with prisms inserted to compensate for the group velocity dispersion.

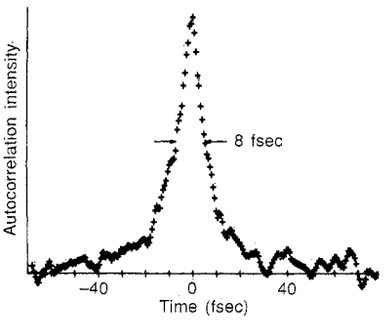

Fig. 2. Measured autocorrelation function of a compressed optical pulse with a full-width at half-maximum of 8 fsec.

Progress in Pulse Generation

The broad frequency bandwidth required to generate a short optical pulse has been a major source of difficulty in the generation of ultrashort optical pulses. A fixed-phase relationship must be maintained among all the frequencies oscillating in a mode-locked laser to generate a bandwidth-limited short optical pulse. Until recently, the group velocity dispersion in a laser cavity, due to mirrors, gain medium, and the saturable absorber, limited pulse generation in a dye laser cavity. However, a new device for compensating group velocity dispersion in an optical cavity was invented by Fork *et al.* (*10*). The device consists of two pairs of prisms inserted into the optical cavity of the laser. Although a prism is typically made of a positively dispersive material, the prism pair arrangement can produce an adjustable amount of negative dispersion. The optical cavity for a colliding-pulse, passively mode-locked dye laser (*11*) with prisms in the cavity (*12*) is shown in Fig. 1. The dispersion in such a cavity is adjusted by moving one of the prisms normal to the prism base. With this cavity configuration, Valdmanis *et al.* (*12*) were able to generate optical pulses as short as 27 fsec.

The signal-to-noise ratio for measurements made with signal-averaging techniques is enhanced by increasing the repetition rate. Recently, amplifiers that operate at high repetition rates (*2, 13, 14*) have been developed to improve the sensitivity of time-resolved spectroscopic measurements. In one design, a dye amplifier pumped by a copper vapor laser has been used to amplify single 40-fsec optical pulses to an energy of 3 μJ at a repetition rate of 10 kHz (*12*). This is a useful apparatus for performing time-resolved spectroscopy.

Optical pulse compression techniques have provided a means of probing the limits of optical pulse generation. Considerable activity in several laboratories has led to rapid progress. After the reported generation of a 30-fsec optical pulse at AT&T Bell Laboratories (*15*), scientists at Massachusetts Institute of Technology reported producing a 16-fsec pulse (*16*), and those at IBM, a 12-fsec pulse (*14*). Currently the shortest reported optical pulse is 8 fsec, which was reported by researchers at AT&T Bell Laboratories (*1*). With rapid progress of this sort, the question of limits immediately arises. The measured autocorrelation corresponding to an 8-fsec optical pulse is shown in Fig. 2.

The process of compressing optical pulses has been reviewed (*17*). The first step is to pass an optical pulse through a nonlinear medium, in this case, a short piece of optical fiber. The intense optical field rapidly changes the index of refraction seen by the optical pulse and impresses a frequency sweep or "chirp" on the optical pulse. The chirped optical pulse is then passed through a "compressor," which provides the phase delay required to remove the frequency sweep and produce a compressed optical pulse. The pulse was shortened because the spectral bandwidth was increased in the nonlinear frequency chirping process, and the compressor provided the correct phase adjustment to produce a minimum optical pulse width.

The current limit on optical pulse compression is due to less than ideal performance of the compressor. The compressor consists of a pair of parallel gratings (*18*) with variable spacing, which permits the adjustment of the amount of phase compensation. For the large bandwidth required to compress an 8-fsec optical pulse, a pair of gratings induces a phase distortion (*18*) that limits pulse compression to approximately 8 fsec. This represents a "technological limit" rather than a fundamental limit for achieving further pulse reduction. In principle, an ideal compressor could be invented.

Femtosecond Measurement Techniques

The power and range of investigations into the dynamical properties of matter have been greatly enhanced by the development of new measurement techniques. These advances have had an important impact on a wide variety of scientific disciplines. In this section, I have selected what I believe to be some of the most exciting applications of femtosecond measurement techniques. The examples illustrate the utility of these techniques in solid-state physics, chemistry, and biology.

Semiconductor dynamics. The interaction of short laser pulses with semiconductors has been studied by time-resolved transmission (*19*), reflectivity (*20*), ellipsometry (*21*), surface second harmonic generation (*3*), and femtosecond imaging (*4*). In particular, the problem of optically induced phase transitions on silicon has been the subject of extensive interest. Time-resolved reflectivity measurements have shown a rapid increase in surface reflectivity in less than 1 psec when the optical pulse energy reaches some threshold energy, E_{th} (approximately 0.1 J/cm^2). This has been widely interpreted as thermal melting. However, reflectivity is a scalar quantity and cannot provide information about the disorder of the crystal lattice that occurs when a material melts. Ideally, we would like to have a femtosecond x-ray pulse to explore the evolution of structural changes in matter. Such pulses have yet to be developed.

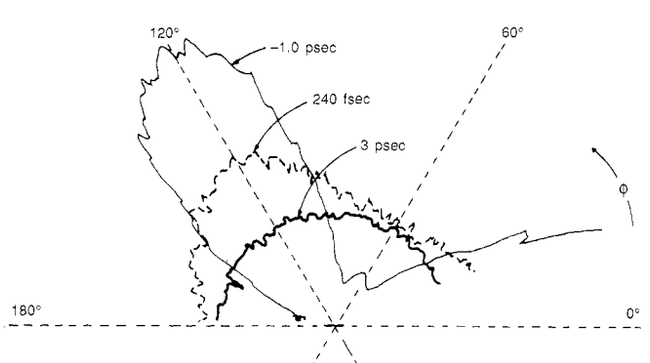

Fig. 3. Polar plot of the surface second harmonic intensity as a function of time and angle for the ⟨111⟩ surface of silicon at an optical pumping energy twice the threshold for melting. The threefold symmetry is lost after the first few hundred femtoseconds as the material melts.

Information about crystal symmetry can be obtained with visible optical pulses by measuring the second harmonic radiation generated at the crystal surface. The second harmonic polarizability is a tensor quantity which can provide information on crystal symmetry (*22*). The ⟨111⟩ surface of silicon has a threefold rotational symmetry in the crystalline state. After silicon melts, the crystal structure becomes disordered and the second harmonic tensor becomes rotationally symmetric.

Figure 3 shows in polar form the second harmonic radiation from the ⟨111⟩ surface of silicon for a weak probing pulse at three relative time delays (*3*). Before the exciting pulse arrives, we see a peaking in the second harmonic at 120° intervals (only a portion of the angular range is plotted), which is consistent with a threefold symmetry. At 240 fsec after excitation the maximum signal is reduced and the signal near the minimum is increased as the crystal begins to disorder. By 3 psec, the material is completely rotationally symmetric, which indicates complete disorder or a transition to the melted state.

Further information can be obtained about the interaction of short laser pulses with semiconductors by using a newly developed imaging technique (*4*). This technique makes it possible to depict the evolution of the surface reflectivity during and after melting initiated with a short optical pulse having a time resolution of 100 fsec and a spatial resolution of 5 μm. In fact, with a movie camera and elementary synchronization electronics, it is possible to film the continuous sequence of melting, boiling, and material ejection over a 600-psec period, slowed in time by as much as a factor of 10^{13}. The still photographs in Fig. 4 depict the major events in this sequence.

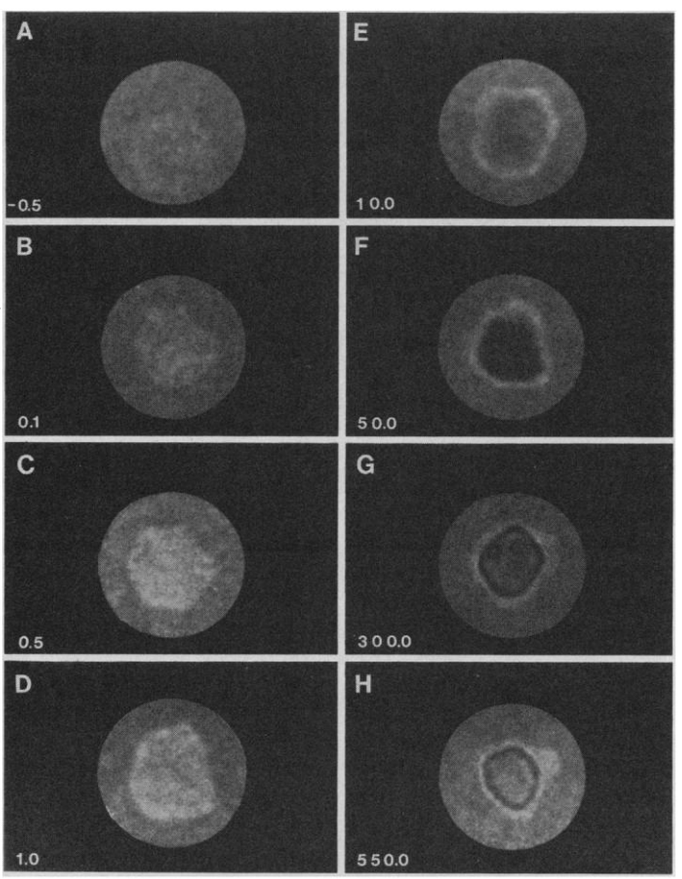

Fig. 4. Time-resolved photographs of a silicon ⟨111⟩ surface after photoexcitation by an 80-fsec optical pulse. The numbers indicate the pump-probe optical delay in picoseconds. Note the rapid appearance of highly reflective molten silicon (B–D) followed by the ejection and dissipation of evaporated material (E–H).

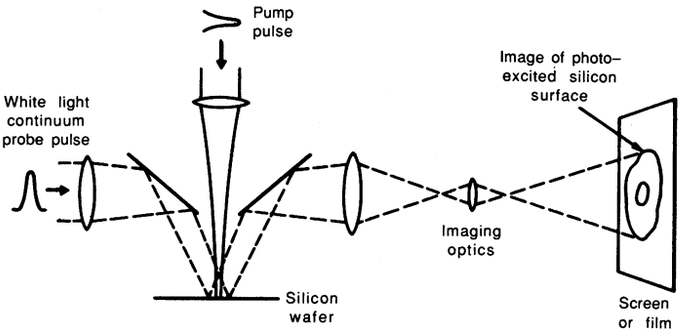

Fig. 5. Experimental arrangement used to obtain femtosecond time-resolved photographic images of a silicon surface undergoing an ultrafast phase transition.

The photographs were obtained with a variation of the pump-and-probe technique. A schematic of the apparatus is shown in Fig. 5. An intense 80-fsec optical pulse was used to excite the silicon wafer surface. A second 80-fsec optical pulse generated from a white light continuum was used to probe the reflectivity of the wafer surface. The image of the photoexcited surface was projected onto a screen or film through the use of imaging optics. The relative timing between pump and probe was adjusted by changing the relative path delay between the two pulses with a stepper motor. The silicon wafer was translated after each laser shot by an electronically controlled stage so that each shot addressed a fresh region of the sample.

The photographs shown in Fig. 4 provide a detailed study of the physics of what is taking place at the semiconductor surface as a function of time after excitation for time delays ranging from −0.5 to 600 psec. Before the arrival of the excitation pulse, only a uniformly illuminated region of the surface is seen in Fig. 4A. After arrival of the excitation pulse, the reflectivity of the excited region is selectively increased because significant melting has occurred in this region. Melting is not complete until nearly 1 psec has elapsed. About 10 psec after excitation, a dark layer begins to form over the melted region. This is consistent with the ejection of liquid drops of silicon forming a strongly scattering cloud. Maximum ejection is expected in the hot central portion of the molten silicon, where the excitation intensity is highest, while the edge remains cool enough that a substantial absorptive cloud never develops. This explains the bright outer ring of unobscured molten silicon that persists throughout the time of observation.

Femtosecond optical techniques offer a unique opportunity to study nonequilibrium phenomena in semiconductors. For direct transitions away from exciton resonances, the absorption coefficient α can be expressed as

$$\alpha = \alpha_o(1 - f_e - f_h)$$

where f_e and f_h are the distribution functions for electrons and holes and α_o is the absorption coefficient in the absence of excited carriers. With a sufficiently short optical pulse, a narrow band of states can be excited to create a nonthermal distribution. As time progresses, carrier-carrier interactions lead to the thermalization of the carrier distribution. Ultimately at much longer times, the carriers equilibrate with the lattice (*23, 24*) by means of electron-phonon interactions.

Newly developed measurement techniques at high repetition rates are ideally suited for nonequilibrium phenomena. A train of femtosecond optical pulses (*11, 12*) amplified to a few microjoules at a repetition rate of 8 Hz is focused into a 1-mm-thick jet of ethylene glycol to generate a femtosecond continuum (*2*). The pulses are split

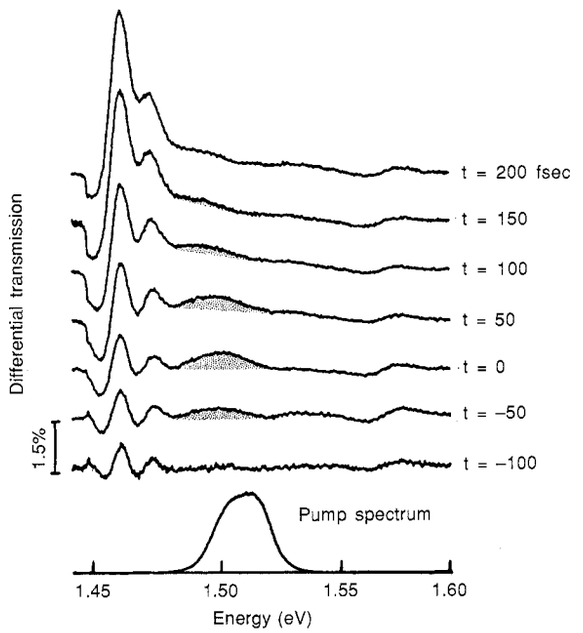

Fig. 6. A plot of differential transmission spectra for a GaAs multiple quantum well after excitation by a pump pulse centered at 1.509 eV. The spectra are plotted at 50-fsec intervals between t = 100 fsec and t = 200 fsec. The pump spectrum is shown at the bottom of the figure. The shaded areas show the effect of "hole" burning by the nonequilibrium nonthermal carrier population.

by a metal beam splitter into pumping and probing pulses. The probing pulses are directed into a spectrometer and detected with a diode array. The relative time delay between the two pulses is provided by a variable path length controlled by a stepper motor.

To detect very small changes in the absorption spectrum, the pumping pulses are chopped with a 10-Hz chopper, and the detected probe spectrum is accumulated in the computer memory with a phase determined by the synchronization with the optical chopper. In this way the differential spectrum is directly accumulated.

Experimental data dramatically demonstrating optical hole burning in a semiconductor by a nonthermal nonequilibrium carrier population are shown in Fig. 6. The sample is a series of thin layers or quantum wells that consist of 65 periods of 96-Å GaAs quantum wells and 98-Å $Al_{0.3}Al_{0.7}As$ barrier layers. The plotted curves are differential transmission spectra. The shaded areas indicate where the transmission spectrum was bleached by the occupation of levels in a narrow energy band. The hole disappears rapidly as the carrier population relaxes to a thermalized distribution. The oscillatory features at low energies are due to perturbations to the light and heavy hole exciton absorptions by the optically excited carriers (*2*).

When the optical pumping pulse is tuned to be resonant with the fundamental exciton absorption, it is possible to directly observe the process of exciton ionization by phonons (*25*). In Fig. 7 a family of differential spectra are plotted as a function of wavelength and time. The sharply peaked feature arises from bleaching of the exciton. As excitons are ionized by the phonon field, the exciton population begins to decay. From these measurements the exciton ionization time is 300 fsec.

Photofragment spectroscopy. Dynamical processes in chemistry have recently become an important area of investigation on the femtosecond time scale. Of particular interest is the report of femtosecond photofragment spectroscopy (*9*). Studies of the dynamics of primary photofragment processes offer new opportunities for a direct view of the process of bond breakage, its dependence on the nature of the transition state, and the resulting energetics of the products. The reaction studied by the group at the California Institute of Technology is

$$\text{I–CN} \rightarrow [\text{I}\text{--}\text{CN}] \rightarrow \text{I} + \text{CN}$$

In the above experiment, a femtosecond optical (photolysis) pulse was used to initiate the photodissociation of ICN to the continuum absorption of the repulsive A state. A second probing pulse was used to monitor the recoiled CN by observing fluorescence from the fragment as a function of relative time delay between the photolysis and probe pulses. The rise time of the measured fluorescence provides a direct measure of time of formation of the CN photoproduct. The measured photoproduct formation time was 600 fsec. Future experiments are expected to provide the details of the transition state in the recoil process.

Impulsive excitation of phonons. Optical techniques have been used extensively to study the dynamics of atomic and molecular vibrations in solids and liquids. Frequency domain techniques, such as infrared absorption spectroscopy and Raman spectroscopy, have provided extensive information about the kinetics of phonons and coupling to elementary excitations in the condensed phase. Optical phonons can be generated and detected coherently by femtosecond techniques. The technique called "impulsive stimulated Raman" spectroscopy requires temporal resolution sufficient to resolve a single phonon oscillation.

The process of "impulsive Raman scattering" has been described by DeSilvestri *et al.* (*6*). Two ultrashort optical pulses were used to excite counterpropagating phonons to form a standing vibrational wave with wave vector $\pm\mathbf{k}$. The phonon frequency was derived from the uncertainty-limited spectral width of the excitation pulses. The optic-vibrational standing wave coherently scattered the delayed probe pulse, which is incident at the phase-matching angle. With a pulse duration of less than 100 fsec, optic phonons having frequencies of up to 200 cm^{-1} can be investigated. The amplitude of the standing wave is then measured as a function of time by varying the relative delay with respect to the excitation pulse. Thus, simultaneous measurements of phonon frequency and damping can be made with high spectral and temporal resolution.

Cheung and Auston have used the Cherenkov radiation geometry (*26*) to induce coherent phonon polaritons to lithium tantalate (*27*) (Fig. 8). The damped oscillation on the trailing edge of the main

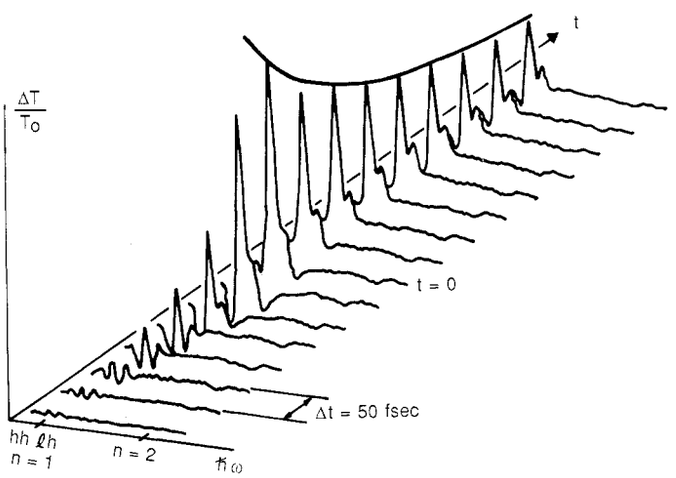

Fig. 7. Plot of time-resolved spectra near the fundamental band edge of a semiconductor GaAs multiple quantum well. The sharp structure is due to bleaching of the band edge excitons. The relaxation of this bleaching is a measure of the time for the process of ionization of the excitons by the phonon interaction and is 300 fsec by this measurement.

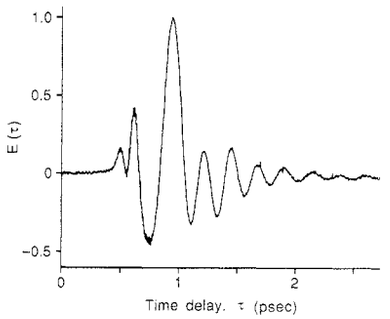

Fig. 8. Polariton waveform in lithium tantalate generated and measured by femtosecond optical pulses. The damped oscillation of the trailing edge of the main pulse is due to the resonant contribution of the second order nonlinear optical susceptibility from the TO phonon at 6 THz.

pulse is due to the resonant contribution to the second order nonlinear optical susceptibility from the TO phonon at 6 THz. These measurements establish that the intrinsic speed limit for the electrooptic effect in this material is limited by the phonon dephasing time of 280 fsec.

Optical ranging through biological material. It was recognized more than a decade ago, after the development of ultrashort optical pulse techniques, that such a pulse in conjunction with a high-speed shutter could be used to investigate the internal structure of turbid media without interference from scattered light (*28*). Duguay and Mattick suggested that it might even be possible to "see through skin." The basic concept is that light reflected and scattered from skin obscures our vision of the tissue just under the skin. With a light shutter it is possible to gate out this reflected light and, by properly timing the shutter, range into the tissue.

Fujimoto *et al.* (*5*) have succeeded in ranging through biological samples with a 15-μm spatial resolution through the use of femtosecond optical pulses. A 65-fsec optical pulse was divided into a reference and a probe pulse with a beam splitter. The probe pulse was focused onto the sample under study, and the reference pulse was focused into a frequency summing crystal along with the light reflected from the sample. The reference and the signal were correlated in the nonlinear mixing process. The integrated sum frequency harmonic energy S as a function of the temporal delay, τ, between the signal and reference yields the cross-correlation

$$S(\tau) = \int I_s(t) I_r(t - \tau) dt$$

where I_s is the signal intensity and I_r is the reference intensity.

Since the sum frequency is proportional to the product of I_s and I_r, weak signals may be detected by using a comparatively strong reference intensity. The detection limit was 10^{-7}. An example of ranging through the skin is shown in Fig. 9 (*5*). The junction between the various tissue types is clearly seen. It appears possible that this technique may be useful to noninvasively monitor pathological processes as well as therapeutic laser tissue interactions.

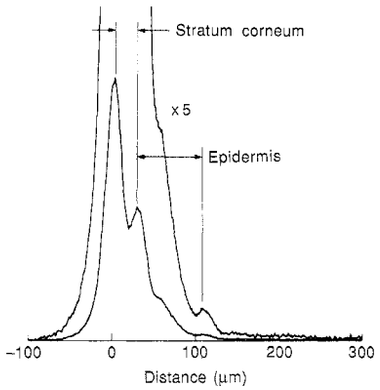

Fig. 9. Optical ranging measurement through human skin.

Conclusion

The diversity of applications of femtosecond optical pulse techniques continues to grow. Time is an important coordinate in almost any scientific investigation. Optical pulsewidths have moved near the limit for investigations in the visible region of the spectrum. The major advances to come in this field will be measured by the impact on the broad spectrum of science.

REFERENCES AND NOTES

1. W. H. Knox *et al.*, *Appl. Phys. Lett.* **46**, 1120 (1985).
2. W. H. Knox, M. C. Downer, R. L. Fork, C. V. Shank, *Opt. Lett.* **9**, 12 (1984).
3. C. V. Shank, R. T. Yen, C. Hirlimann, *Phys. Rev. Lett.* **51**, 900 (1983).
4. M. C. Downer, R. L. Fork, C. V. Shank, *J. Opt. Soc. Am. B* **2**, 595 (1984).
5. J. G. Fujimoto *et al.*, *Opt. Lett.* **11**, 150 (1986).
6. S. DeSilvestri *et al.*, *Chem. Phys. Lett.* **116**, 146 (1985).
7. J. Valdmanis and G. Mourou, *IEEE J. Quantum Electron.* **QE-22**, 69 (1986).
8. B. Kolner and D. Bloom, *ibid.*, p. 79.
9. N. F. Scherer, J. L. Knee, D. D. Smith, A. H. Zewail, *J. Phys. Chem.* **89**, 5141 (1985).
10. R. L. Fork, O. E. Martinez, J. P. Gordon, *Opt. Lett.* **9**, 150 (1984).
11. R. L. Fork, B. I. Greene, C. V. Shank, *Appl. Phys. Lett.* **38**, 671 (1981).
12. J. A. Valdmanis, R. L. Fork, J. P. Gordon, *Opt. Lett.* **10**, 131 (1985).
13. I. N. Duling III, T. Norris, T. Sizer II, P. Bado, G. A. Mourou, *J. Opt. Soc. Am. B* **2**, 616 (1985).
14. J. M. Halbout and D. Grischkowsky, *Appl. Phys. Lett.* **45**, 1281 (1984).
15. C. V. Shank, R. L. Fork, R. Yen, R. H. Stolen, W. J. Tomlinson, *ibid.* **40**, 761 (1982).
16. J. G. Fujimoto, A. M. Weiner, E. P. Ippen, *ibid.* **44**, 832 (1984).
17. C. V. Shank, *Science* **219**, 1027 (1983).
18. E. B. Treacy, *IEEE J. Quantum Electron.* **QE-5**, 454 (1969).
19. C. V. Shank, R. L. Fork, R. F. Leheny, J. Shah, *Phys. Rev. Lett.* **42**, 112 (1979).
20. C. V. Shank, R. Yen, C. Hirlimann, *ibid.* **50**, 454 (1983).
21. D. H. Auston and C. V. Shank, *ibid.* **32**, 1120 (1974).
22. N. Bloembergen, R. K. Chang, S. S. Jha, G. H. Lee, *Phys. Rev.* **174**, 813 (1968).
23. J. L. Oudar *et al.*, *Phys. Rev. Lett.* **53**, 384 (1984).
24. W. H. Knox *et al.*, *ibid.* **56**, 1191 (1986).
25. W. H. Knox *et al.*, *ibid.* **54**, 1306 (1985).
26. D. H. Auston, K. P. Cheung, J. A. Valdmanis, D. A. Kleinman, *ibid.* **53**, 1555 (1984).
27. K. P. Cheung and D. H. Auston, *ibid.* **55**, 2152 (1985).
28. M. A. Duguay and A. T. Mattick, *Appl. Opt.* **10**, 2162 (1971).